Deuteron breakup at 2.1 and 1.25 GeV

V. Punjabi,* C. F. Perdrisat, P. Ulmer, and C. Lyndon
College of William and Mary, Williamsburg, Virginia 23185

J. Yonnet, R. Beurtey, M. Boivin, and F. Plouin
Laboratoire National Saturne, 91191 Gif-sur-Yvette, France

J. P. Didelez, R. Frascaria, T. Reposeur, R. Siebert, and E. Warde
Institut de Physique Nucleaire, 91410 Orsay, France

A. Boudard
Département de Physique Nucléaire, Moyennes Energies, Centre Etudes Nucléaires, Saclay, 91191 Gif-sur-Yvette, France

P. C. Gugelot
University of Virginia, Charlottesville, Virginia 22901
(Received 17 October 1988)

Inclusive differential cross section and analyzing power T_{20} in $A(d,p)X$ at 2.1 GeV and for protons at 0° are presented for the targets ^{1}H, ^{4}He, ^{12}C, Ti, and Sn. In addition, data for ^{1}H at 1.25 GeV are also shown. For all targets the cross-section data show a similarity in shape when plotted as a function of q, the proton momentum in the deuteron frame, each target exhibiting a shoulder near $q=0.30-0.35$ GeV/c. Likewise, T_{20} values are largely independent of the target's A value. When compared with higher-energy data for ^{12}C$(d,p)X$, the new results establish the universality of the shoulder over the energy range 1.25–7.4 GeV, as well as the energy independence of T_{20}. The ^{1}H$(d,p)X$ data are compared with the results of a nonrelativistic calculation of the six lowest-order graphs of the process using elastic, on-shell NN amplitudes and the Paris NN potential deuteron wave function. The calculated cross sections have no shoulder at either of the two energies of this experiment; the observed behavior of T_{20} is reproduced qualitatively only. Comparisons with ^{2}H$(p,2p)$ and ^{2}H$(e,e'p)$ data are made and various possible origins for the anomalous shoulder discussed, including π rescattering, Δ excitation, and a six quark component in the deuteron.

I. INTRODUCTION

Deuteron breakup at high energy is, in first approximation, a relatively simple process in which one of the nucleons of the deuteron is removed in a small momentum transfer to the target and the other nucleon proceeds largely undisturbed; hence the nature of the target is expected to play only a minor role. In this simplified description, which is compatible with data obtained in the early days of the impulse approximation (IA), the velocity of the detected proton is the one it had prior to the breakup. The inclusive differential cross section $d^2\sigma/d\Omega_p dp$ for the $A(d,p)X$ breakup process on a target of atomic number A, is then directly proportional to the deuteron single-nucleon momentum density $|\Phi(q)|^2$ and independent of A, other than for a scale factor. With these assumptions the only variable of physical interest is the proton momentum in the deuteron rest frame, obtained by Lorentz transformation of the proton laboratory momentum; this variable will be called q here.

Several experimental results have confirmed the IA picture for small internal momenta of the proton in the deuteron. However, higher-energy cross section results[1,2] for 0° protons have shown a marked deviation from the IA prediction at values of q larger than 0.2 GeV/c. In a recent paper[3] data were presented which indicated that this deviation, in the form of a relatively broad shoulder, systematically occurred at a value of $q\approx 0.3$ to 0.35 GeV/c, and for deuteron kinetic energies ranging from 2.1 to 7.2 GeV; the target was ^{12}C, with additional data for hydrogen and Ti showing the same effect. In Ref. 3 the tensor analyzing power T_{20} was also presented and found to agree with the simplest IA prediction up to $q\approx 0.2$ GeV/c, and then markedly deviate from it at larger q values.

Several explanations for these deviations from the IA prediction are possible. First of all, one must ascertain whether the anomalous shoulder is not simply a deviation from the IA due to multiple scattering of the participating nucleons. Also the role of pions must be evaluated; for these data and those in Refs. 1–3, for parts of the proton spectrum the missing energy is large enough to allow for one or more pions to be present in the final state. In this range the Δ resonance is known to play an important role, either on or off the mass shell. It has also been pointed out that relativistic effects might have to be considered in this energy range.[4] An interesting question is whether high-energy deuteron breakup truly reveals de-

tails of the deuteron structure which have not been detected unambiguously so far. It has been suggested in Ref. 3 that a colorless six-quark state in the deuteron might be at the origin of the shoulder. The consequences of such a component, as well as a $\Delta\Delta$ component, on both cross section and T_{20} analyzing power were also discussed in Ref. 3.

The data presented here include differential cross section and T_{20} for 0° protons of momentum between half the beam momentum and the maximum allowed by kinematics. Data with better statistics than in Ref. 3 have been obtained for the targets ^{1}H, ^{12}C, Ti, and new data for ^{4}He and Sn, all at 2.1 GeV in a continuation of the experiment in 1987. In addition, ^{1}H data at 1.25 GeV are presented. The data for hydrogen will be compared with the results of a nonrelativistic calculation which is an extension of one undertaken recently for 0.508 GeV ^{2}H$(p,2p)n$ data[5] and does not include pion production or absorption. It is an evaluation of the first- and second-order graphs of a multiple scattering expansion and is a continuation of the work of Ref. 5 to obtain inclusive differential cross sections and T_{20}. The calculation requires elastic NN amplitudes, and for these the phase-shift analysis results of Arndt *et al.*[6] [Virginia Polytechnical Institute (VPI) phase-shift amplitudes] have been used. The np amplitudes are determinant for the result, and unfortunately these are least well known in the energy range of interest here, as was recently reemphasized by Arndt[7] in a comparison with the Saclay phase shifts.[8] Therefore, the results of the calculation suffer from large uncertainties, most of all for polarization observables. Nevertheless they indicate that the observed cross-section shoulder at constant q is most likely not a rescattering or final-state interaction effect. The T_{20} data cannot be reproduced with a satisfactory level of confidence at this time, unless the double-scattering contribution involving two np interactions is left out. Most recently Ignatenko and Lykasov[9] have presented evaluations which indicate that pion production may be responsible for part of the shoulder in Ref. 1. They argue that an excess of cross section in the new data of Azhgirei *et al.*[10] for breakup at large proton transverse momenta may be explained with pion production. The much lower energy of the present data, and the similarity of the shoulder observed at all energies between 1.25 and 7.2 GeV suggest to us that pion production is probably not the explanation.

In Sec. II, experimental details not discussed in Ref. 3 will be presented. The data analysis will be described and the results presented in Sec. III. The calculation in IA and of rescattering graphs will be reviewed in Sec. IV, where the data for breakup on hydrogen at deuteron energies of 2.1 and 1.25 GeV will be compared to the prediction. The experimental results, comparison with other results and their interpretation will be reviewed and conclusions presented in Sec. V.

II. EXPERIMENT

Polarized deuteron beams of 2.1 and 1.25 GeV accelerated by the synchrotron Saturne 2 in the Laboratoire National Saturne at Saclay were directed on various targets viewed by the spectrometer SPES IV. The recently commissioned injector MIMAS provided polarized deuterons in excess of 10^{11} per burst. The SPES IV facility allows 0° detection with an additional dipole magnet at the spectrometer entrance to deflect particles scattered at 0° into the entrance collimator by an angle of $\approx 7.5°$, assuring separation of scattered particles from beam particles as long as their magnetic rigidities are not the same. The resolution of the spectrometer in the large acceptance mode is typically 10^{-3}, and the momentum acceptance $\pm 3\%$ for the solid angles used in this experiment ($\Delta\Omega_p = 0.0192$ and 0.0988 msr, respectively, depending on the size of the cross section being measured). Further details on the spectrometer can be found in Grorud *et al.*[11]

Targets on a ladder and under vacuum included cryogenic cells with liquid hydrogen and liquid helium-4, and solid targets of graphite (^{12}C), Ti, and Sn. The target thicknesses were 0.1012 and 0.2641 g cm^{-2} for ^{1}H, 0.47 g cm^{-2} for ^{4}He, 1.97 g cm^{-2} for C (graphite), 3.21 g cm^{-2} for Ti (natural), and 3.20 g cm^{-2} for Sn (natural). Thickness uncertainties are ± 0.0035 g cm^{-2} for the liquid targets, and $\pm 3\%$ for the solid targets, respectively.

Under the conditions of this experiment, the beam deflected by the entrance dipole was stopped near the collimator, increasingly close to the solid angle defining aperture as the tuned momentum approached the beam momentum. The largest proton momentum for which separation between protons and background deuterons is possible depends upon the size of the cross section of interest. The 40-cm thick lead collimator does not stop beam or scattered deuterons; as a result, for the proton momenta close to the beam momentum, a sizable background of particles originating at the collimator, with velocities close to that of the beam deuterons, was observed. However, SPES IV provides excellent mass separation. The total length of the spectrometer is about 35 m, with 16 m between intermediate and final focal planes used for time-of-flight measurements; the time-of-flight separation between protons and deuterons is shown in Fig. 1. A detailed description of the detector package used in this experiment, not including the Cerenkov detectors, can be found in Ref. 12. As shown here schematically in Fig. 2, a 12-element hodoscope in the intermediate focal plane (I), and a 13-element hodoscope in the final focal plane (F) helped select allowed trajectories using the tight position-angle correlation of the trajectories. Included in a "slow" trigger are only hodoscope element combinations (I_iF_j) which are optically allowed. A tightly adjusted "fast" trigger was formed between pulses of the I telescopes and two large scintillator paddles (L) located behind the drift chambers in the final focal plane area, to constrain the "slow" trigger further with a gate 3 ns wide; this was an addition to the trigger of Ref. 3. Furthermore, Cerenkov light pulses from four plastic rods[13] located at the rear of the detector package were required to validate the trigger further when needed to help reject background events, consisting mostly of stray deuterons. The index of refraction $n = 1.49$ of the rods resulted in the Cerenkov light produced by undesirable deuterons not being internally reflected in the plastic rods, and thus

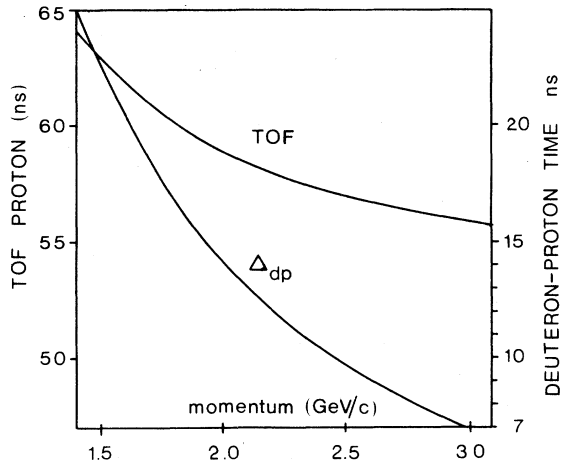

FIG. 1. Time of flight for protons and deuterons in SPES IV, showing the time separation Δ_{dp} available over the momentum range of interest.

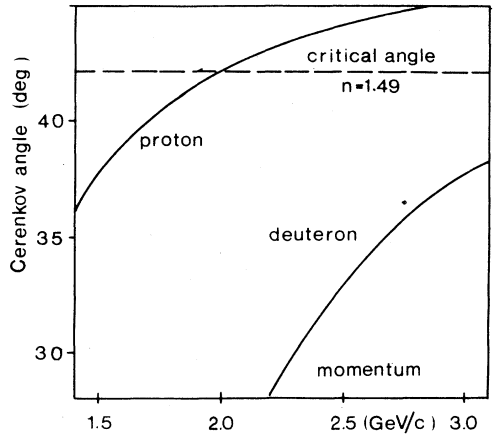

FIG. 3. Angle of the Cerenkov light cone for the protons and deuterons in the momentum range of this experiment. Light emitted at less than the critical internal reflection angle of 42.16° is not transmitted to the end phototubes.

not reaching the photomultipliers at either ends of the rods. Figure 3 shows the Cerenkov light-angle separation for the two particles versus the momentum setting of the spectrometer.

The position information from the two *XXY*-coordinate transverse drift chambers were used to reconstruct the particle trajectories at the location of the collimator, and help reject background events, as well as to calculate the particle momentum using the known first-order (and second-order) transport matrix coefficients. Additional time-of-flight and pulse height cuts were applied off line when the background conditions required it.

The beam monitors were the same as described in Ref. 3; again the main monitors were a secondary electron monitor (SEM) and an ionization wire chamber ($D3$) modified to collect the charge freed by the incoming deuterons. Two coincidence telescopes from the high-energy polarimeter in the SPES IV beam line viewing a thin auxiliary target located upstream of the main target

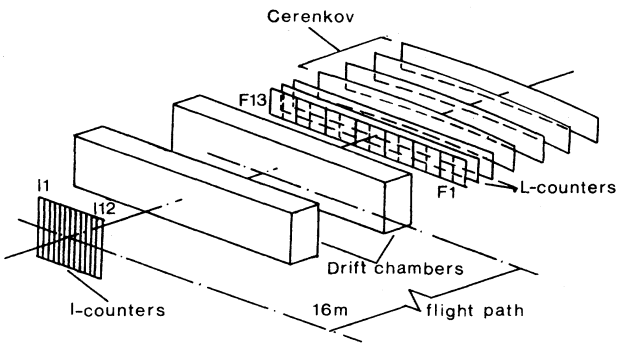

FIG. 2. Detection of SPES IV as used in present experiment, showing the I counter telescope in the intermediate focal plane, two *XXY*-coordinate drift chambers, followed by the F counters near the final focal plane, the two L scintillators required in the fast trigger, and four internal reflection Cerenkov detectors.

were scaled both free and gated by the computer to measure the experimental dead time.

In the polarized mode successive beam bursts contain deuterons in periodically changing polarization states numbered 5–8 and characterized by vector and tensor polarizations changing from $\rho_{10}=+1/\sqrt{6}$ and $\rho_{20}=+1/\sqrt{2}$, to $-1/\sqrt{6}$ and $+1/\sqrt{2}$, $+1/\sqrt{6}$ and $-1/\sqrt{2}$, and finally $-1/\sqrt{6}$ and $-1/\sqrt{2}$. Beam bursts 1–4 can be used when optimum vector, rather than tensor polarization is required. Additional information on the polarized deuteron beams at Saturne are found in Arvieux *et al.*[14]

The unpolarized cross section $d^2\sigma/d\Omega_p dp$ is obtained by adding the events in the four polarization states. Tensor and vector asymmetries are defined as

$$X_T=(n_7+n_8-n_5-n_6)/(n_5+n_6+n_7+n_8)\,,$$

and (1)

$$X_V=(n_5-n_6+n_7-n_8)/(n_5+n_6+n_7+n_8)\,,$$

where the n_i's are the numbers of events corrected for unequal numbers of deuterons in each polarization state and for different dead times of the experimental setup in each state. At a scattering angle of exactly 0° the differential cross section for purely tensorially polarized deuterons depends exclusively upon the tensor analyzing power T_{20}, the other tensor analyzing powers being zero for symmetry reasons. Although neither data nor theoretical prediction exist for T_{22} near 0°, it must have a zero derivative relative to the scattering angle; furthermore, the small beam divergence and spectrometer acceptance centered at 0° are additional justifications to neglect these terms. The beam divergence at the target was ±4 mr horizontally and vertically; the spectrometer angular acceptance was ±2.5 and ±5.6 mr both horizontally and vertically, for the small and large solid angles, respectively. With the direction of quantization vertical and fol-

lowing the Madison convention, the differential cross section is

$$(d\sigma/d\Omega_p dp)_{\rm pol}=(d^2\sigma/d\Omega_p dp)_{\rm unpol}(1-\rho_{20}T_{20}/2)\ , \tag{2}$$

where T_{20} is related to the measured tensor asymmetry X_T defined in (1) by $T_{20}=2X_T/\rho_{20}$; ρ_{20} is the polarization of the beam, which was determined in Ref. 3 to be 0.877 ± 0.014 times the theoretical value of $1/\sqrt{2}$. Equipment failure in 1987 prevented a remeasurement of the polarization in the injector line; the breakup data from the two years, measured under identical conditions, indicate that the beam polarizations differed by less than ±0.01.

III. EXPERIMENTAL RESULTS

A. Differential cross section

The present investigation of the $A(d,p)x$ reaction was originally motivated by a report by Ableev *et al.*[1] of an anomaly in the 0° proton cross section for 7.2-GeV deuterons. These results are shown in Fig. 4(a), where the invariant inclusive differential cross section $(E_p/^2)d^2\sigma/d\Omega_p dp$ is displayed vs q, the proton momentum in the deuteron frame calculated from the proton laboratory momentum p by

$$q=\gamma p-\eta E_p\ , \tag{3}$$

where

$$(\gamma,\eta)=(E_d,\mathbf{d})/m_d\ .$$

$(E_p,\mathbf{p})$ is the four-momentum of the proton. Also shown in Fig. 4(a) are the data of Anderson *et al.*[2] for the same reaction but for 4.2-GeV deuterons and our 2.1-GeV data from Ref. 3; in all three cases the target is carbon. The anomalous shoulder noticed first in Ref. 1 is near $q=0.35$ GeV/c. The curve in the figure is calculated as described in Ref. 1, for the deuteron wave function of the Paris NN potential.[15]

All invariant differential cross-section results from the present experiment at 2.1-GeV deuteron energy are shown vs q in Fig. 4(b); included also are the hydrogen and carbon results of Ref. 3. For most points the statistical error bars are too small to be visible. For the new data, the systematic uncertainty is the same for all values of q, approximately $\pm5\%$.

The new data in Fig. 4(b) confirm and strengthen the results of Ref. 3. Comparison with the higher-energy data in Fig. 4(a) leads to the following remarks. A shoulder definitely exists in all 2.1-GeV spectra, always near a value of $q\approx0.30$ to 0.35 GeV/c for all targets, much the same as seen at higher energies in Fig. 4(a). The shape of all cross-section results, perhaps with the exception of hydrogen, is very nearly the same. For carbon the shape remains the same over the range of energies covered in Figs. 4(a) and 4(b), 2.1–7.2 GeV. This independence in shape for both projectile energy and target is a striking property of the reaction.

Whether the anomalous shoulder has its origin in a feature of the deuteron structure cannot be decided simply on the basis of these differential cross-section data, without a comparison with the prediction of a model of the reaction. However, it is a model-independent fact that a shoulder with similar characteristics is present for all five targets, and for carbon at energies of 2.1, 4.2, and 7.2 GeV.

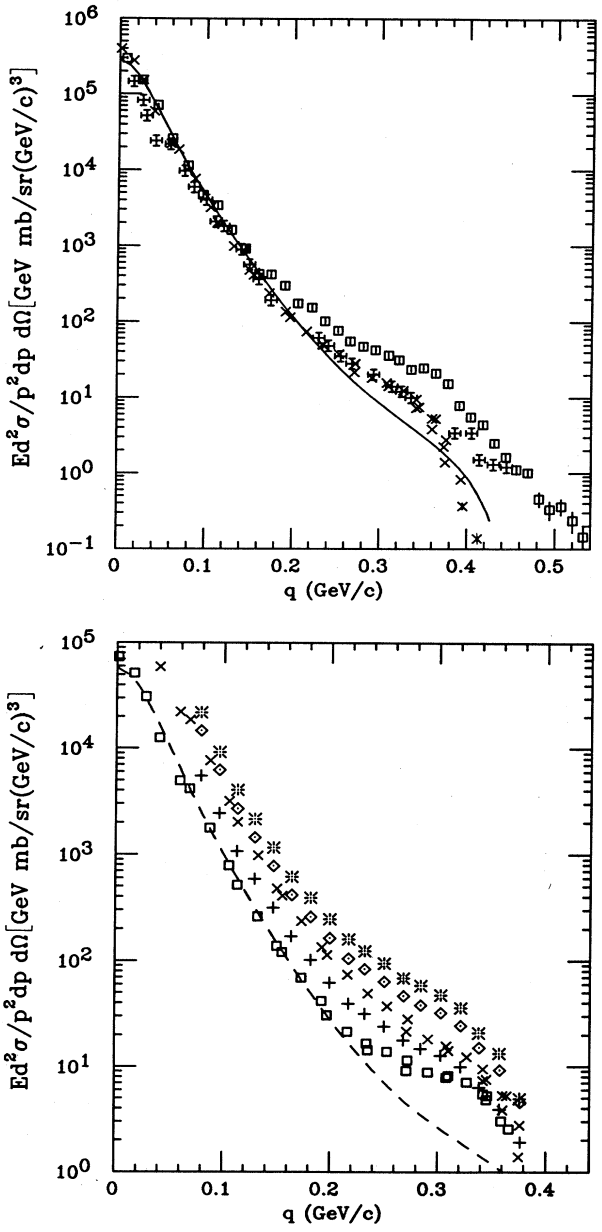

FIG. 4. (a) Comparison of the $^{12}C(d,p)X$ data for 0° protons in the experiment of Ref. 1 at 7.2 GeV (□), the 4.2-GeV data of Ref. 2 (⊕) and the present data (×) at 2.1 GeV. The shoulder near $q=0.30$–0.35 GeV/c is visible in all three data sets. The solid curve calculated was as in Ref. 1 for Paris NN potential wave function (no six-quark component). (b) The inclusive differential cross section at 2.1 GeV for ^{1}H(□), ^{4}He(+), ^{12}C (×), Ti (◇), and Sn (∗). Notice the shoulder near $q=0.30$–0.35 GeV/c for all five targets.

In Fig. 5 the ratios of the differential cross sections for ^{1}H, ^{12}C, Ti, and Sn to ^{4}He are shown vs q. The data points are all from the 1987 experiment; they have been obtained at the same proton lab. momenta for all targets. The q values are the same for all targets because q as defined in (3) is independent of the mass of the target. It is obvious that the cross-section ratios in Fig. 5 for Sn, Ti, and ^{12}C to ^{4}He are nearly constant, again suggesting that the shoulder is a property of the deuteron rather than the target. In addition, in Fig. 5 the ^{1}H data of Ref. 3 are shown as a dot-dashed line; they were taken at different values of the proton momentum but at the same deuteron energy. The shoulder remains in the ratio, indicating that it is relatively stronger in ^{1}H than in the four other targets.

The differential cross-section data for hydrogen at 1.25 GeV will be shown and discussed together with the 2.1-GeV points in Sec. IV in relation to the results of the IA and rescattering calculations.

B. Analyzing power T_{20}

The results of the first measurement of T_{20} for the inclusive deuteron breakup reaction $A(d,p)X$ were published in Ref. 3. In Fig. 6(a) new results are shown for the same five targets as in Sec. III A. These data have significantly smaller error bars than the earlier results for hydrogen and carbon, which are also included in Fig. 6(a). The error bars shown are statistical only. They have been calculated from

$$\Delta T_{20}=2[(1-X_T^2)/N]^{1/2}/\rho_{20}\ , \tag{4}$$

where N is the total number of events observed in the four polarization states, X_T is the tensor asymmetry defined earlier, and ρ_{20} is the beam tensor polarization. The systematic uncertainty on each point is estimated to be ± 0.025.

Here again, as with the differential cross sections, one observes little change in the behavior of T_{20} from one tar-

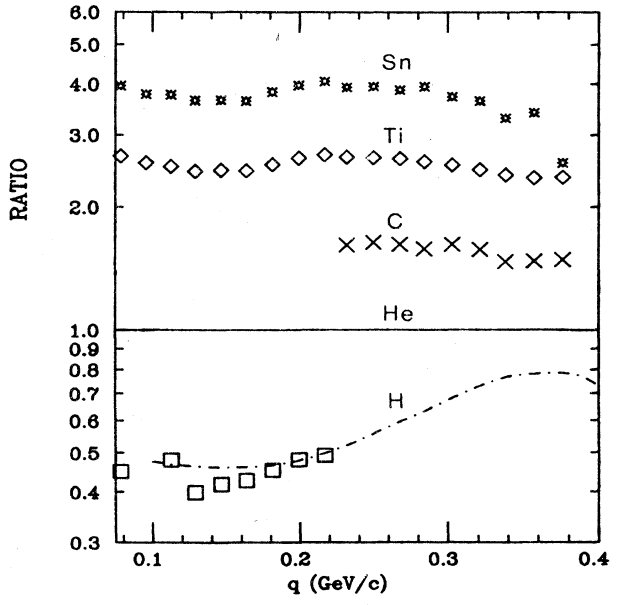

FIG. 5. Ratio of the differential cross sections from the various targets to ^{4}He; the symbols are (*) for Sn, (◇) for Ti, (×) for ^{12}C, and (□) for ^{1}H. The ^{1}H data of Ref. 3 are represented by the dot-dashed curve because they were not taken at the same proton momenta as the new data.

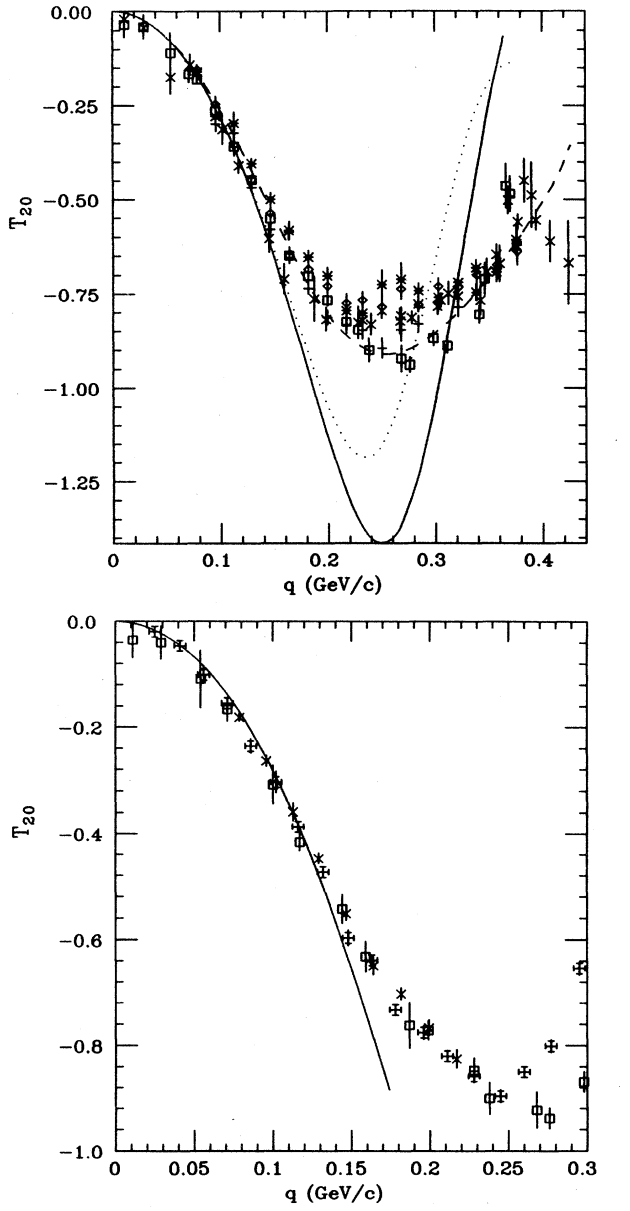

FIG. 6. (a) The analyzing power T_{20} for the same five targets as in Fig. 4(b): Sn (*), Ti (◇), ^{12}C (×), ^{4}He (+), and ^{1}H(□). Also included are the results of Ref. 3 for ^{1}H and ^{12}C. The solid curve is the geometric estimate for the Paris wave function. The dotted curve includes the addition of a $\Delta\Delta$ component and the dashed curve is for the hybrid wave function used by Ableev *et al.* with a $|6q\rangle$ probability of 4% (see Ref. 3 for further details). (b) The analyzing power T_{20} for ^{1}H at 2.1 GeV (□) for 1986 and (×) for 1987, and 1.25 GeV (✠), shown magnified. The solid curve is the geometric prediction for the Paris deuteron wave function.

get to another; all results are within a narrow band up to $q=0.2$ GeV/c. Some target dependence is seen above this q value; hydrogen shows the largest analyzing power, tin the smallest. Recent data[16] for T_{20} in $^{12}C(d,p)X$ at 0.4° and 7.4-GeV deuteron energy are compatible within experimental uncertainties with the ^{12}C data of the present experiment, demonstrating a surprising *energy* independence for T_{20} as well.

Within the limitations of the simplest IA description of the reaction, the q dependence of T_{20} is entirely determined by the momentum space deuteron wave function. If, as for the cross section, one assumes that the breakup probability is simply proportional to the momentum space single-nucleon density, then

$$\begin{aligned}\sqrt{2}T_{20}&=[d\sigma(M=+1)+d\sigma(M=-1)\\&\quad-2d\sigma(M=0)]/(d\sigma)_{\text{unpol}}\\&=[2\sqrt{2}\Phi_D(q)\Phi_S(q)-\Phi_D^2]/\Phi^2\ ,\end{aligned}\tag{5}$$

where $d\sigma(M)$ is the differential cross section for a given projection M of the deuteron total angular momentum J along the quantization direction (here parallel to the accelerator magnetic field, i.e., vertical); Φ_S, Φ_D, and Φ^2 are the deuteron momentum space wave functions for the S and D state, and the total density, respectively. In this extreme simplification the origin of T_{20} is geometrical, being entirely due to the nonsphericity of the deuteron. Thus, the geometrical estimate of T_{20} is energy as well as target independent. Furthermore the geometrical estimate has a minimum equal to the physical limit of $-\sqrt{2}$ which occurs when the ratio of the D- and S-state wavefunction amplitudes is $-\sqrt{2}$. However, the most negative experimental T_{20} value was reported to be -0.920 ± 0.025 in Ref. 3 for hydrogen, in poor agreement with the geometric prediction.

In Fig. 6(a) the solid curve corresponds to the geometric prediction calculated with the Paris deuteron wave function. The dashed curve and the dotted curve are also geometric and are taken from Ref. 3; they correspond to the hybrid wave function of Ref. 1 with a 4% $6q$ component and to wave function with a 5% $\Delta\Delta$ component, respectively.

In Fig. 6(b) the low-q part of the hydrogen T_{20} data at 2.1 GeV (Ref. 3) and all new 1.25-GeV data are shown. No energy dependence is visible within experimental uncertainties. The geometric prediction with the Paris NN potential deuteron wave function is very close to the data up to $q\approx0.13$ GeV/c. The discussion of the hydrogen T_{20} results will be continued in Sec. IV.

IV. MULTIPLE-SCATTERING DESCRIPTION OF $^1H(d,p)X$

In order to find out whether the anomalous shoulder discussed in Sec. III is simply a deviation from the IA due to rescattering or final-state interaction (FSI), the original calculation of Wallace[17] for $^2H(p,2p)n$ with symmetric kinematics has been adapted to the conditions of the inclusive and time-reversed reaction $^1H(d,p)np$. The calculation is based on a Glauber multiple-scattering expansion[18] and is nonrelativistic. In a first step Wallace's formalism was extended[19] to arbitrary (nonsymmetric) kinematics for comparison with the $^2H(p,2p)n$ data of Punjabi *et al.*[20] A further extension to the $^1H(d,p)np$ reaction of interest here was then made and the inclusive differential cross section and analyzing power T_{20} obtained.

The six graphs included in the calculation are in Fig. 7; they correspond to first order (the dominant IA with np interaction as well as the IA with pp interaction) and second order (four graphs with two NN interaction vertices each, $\nu=1-4$ in the figure). All graphs are evaluated with *elastic* and *on-shell* np and pp amplitudes; pion production is not taken into account. The singlet and triplet NN amplitudes defined by Stapp *et al.*[22] and used in Ref. 17 were calculated from the phase-shift analysis amplitudes of Arndt *et al.* (Ref. 6). The Paris NN potential deuteron wave function[21] was used. Neither the NN amplitudes nor the wave function are relativistically invariant; however, all kinematics are treated relativistically. The calculation contains no free parameters, but the required on-shell amplitudes are quite uncertain in the energy domain of the present experiment, most severely for np polarization observables (see Ref. 7).

The unpolarized exclusive $(p,2p)$ differential cross section is written in terms of a three-body T matrix which includes a coherent sum over the six lowest-order graphs:

$$d^3\sigma/d\Omega_3 dp_4 d\Omega_4=(K/6)\sum_{LMS}\langle\,|\mathbf{p}_3,\mathbf{p}_4,\mathbf{p}_5,L|T|\mathbf{O},M;\mathbf{p}_1,S\rangle_A|^2\tag{6}$$

with the elements $T_{LMS}=\langle f|T|i\rangle$ of the total T matrix for the six graphs, given by

$$|T_{LMS}|^2=|T_{LMS}(\mathrm{IA},np)+T_{LMS}(\mathrm{IA},pp)+\sum_{\nu=1}^{4}T_{LMS}^{(\nu)}/4\pi|^2\ ,\tag{7}$$

where ν numbers the second-order graphs in Fig. 7. In (6) K is a kinematic factor, S is the spin projection ($\pm\frac{1}{2}$) of the incoming proton of momentum $\mathbf{p}_1$, M is the projection of the deuteron total angular momentum ($+1,0,-1$), and L is one of the eight independent spin states for a three-nucleon system; the factor $\frac{1}{6}$ arises from averaging over the initial spin states and A indicates that final-state wave functions have to be antisymmetrized in the two protons. The final-state nucleons have momenta $\mathbf{p}_3$, $\mathbf{p}_4$, and $\mathbf{p}_5$. The details of the reduction of the three-body T matrix in (6) to two-body matrix elements are given in Refs. 5 and 19. The exclusive cross section in (6) was then integrated over the solid angle of one of the final-state protons for each one of the three M states of the deuteron to obtain the analyzing power T_{20}. The invariant form of the cross section for each of the M states is

$$\frac{E_4 d^2\sigma(M)}{p_4^2 d\Omega_4 dp_4} = \frac{1}{2p_1}\int p_3^2 s_{34} \sum_{L,S} |T_{LMS}|^2 / |E_5 p_3 - E_3 p_5 \cos\Theta_{35}| d\Omega_3 \ . \tag{8}$$

Note that in (8) the summation is over L and S only, and the integration is over the full solid angle of particle 3. The factor $\frac{1}{2}$ is for averaging over the two spin states of the initial-state proton. The integral must be evaluated numerically by calculating the complete kinematics at every step of (Θ_3, ϕ_3). The tensor analyzing power T_{20} can then be calculated from (5) in Sec. III B; the summation over M of (8) divided by 3 is the unpolarized inclusive differential cross section. The invariant cross section in (8) is also the one wanted for ^{1}H$(d,p)pn$ provided it is calculated at the correct value of the total invariant energy squared: $s=(p_d+p)^2$, where p_d and p are the initial-state four-momenta. The integration over solid angle $\Delta\Omega_3$ requires careful treatment of the Jacobian which peaks at the maximum laboratory angle of particle 3.

The dominant contribution for (d,p) comes from the IA graph with np interaction. The amplitudes for the singlet (M_{ss}) and triplet (M_{00} and M_{11}) pp interaction include a Coulomb part; however, including Coulomb amplitudes at all pp vertices leads to disaster as the integral for the inclusive cross section in (8) requires 0° scattering amplitudes which are infinite. The results presented here have been obtained *without* any Coulomb amplitude; this procedure gives a correct estimate for the unpolarized differential cross section. Unreasonable T_{20} values are obtained if one includes a Coulomb part in the pp amplitudes. Although this procedure is *ad hoc*, one does indeed expect that the deuteron is broken mainly by the strong interaction at the large energy of this experiment. A very different situation prevails at low energy (10–100 MeV range), where Coulomb breakup is dominant (Udo[23]).

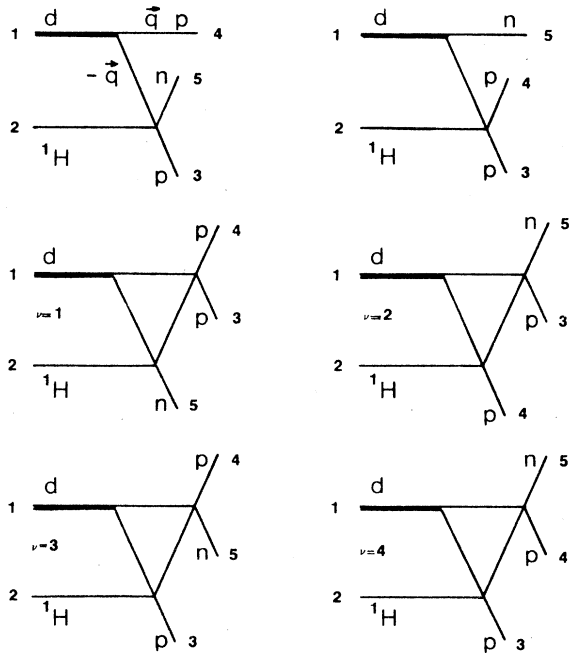

FIG. 7. The first-order (top two diagrams) and second-order Feynman graphs ($\nu=1$–4) calculated in Ref. 19 and integrated to the inclusive differential cross section and T_{20} as described in Sec. IV.

The results of the present calculations are unfortunately strongly limited by the nonavailability of reliable np amplitudes in the high-energy domain of the data. The 1.25-GeV $d\,^1H \rightarrow pX$ data require np and pp amplitudes around $T_p = 0.625$ GeV. However, because the integrals over the triangular part of the double scattering graphs, as well as the integral in (8) over the solid angle $d\Omega_3$ require the wave function of the deuteron out to large values of q for stable results; NN collision energies up to ≈ 0.85 GeV occur in this case. The VPI phase-shift solutions of Ref. 6 do not apply above 1.3 GeV, and, in fact, for the np amplitudes large uncertainties are known to exist already at 0.8 GeV. A recent comparison in Ref. 7 of the VPI (Ref. 6) and Saclay[8] phase-shift solutions for np shows that already between 0.5 and 0.8 GeV some of the np polarization observables predicted by the two solutions differ by up to the size of the observable themselves in some cases. The second calculation was made at $T_p = 1.0$ GeV in the $(p,2p)$ channel, corresponding to 2.0 GeV in the breakup channel; collision energies of up to 1.4 GeV occur in this case, and the results are approximate at best.

As shown in Figs. 8(a) and 8(b), the unpolarized inclusive cross section calculated with all six graphs and with the restrictions and uncertainties described above are in fair agreement with the data both at 1.25- and 2.1-GeV deuteron energies. The general shape of the data is reproduced, but no shoulder is generated by the four rescattering processes included in the calculations. The calculated cross sections differ only by 20% for the two energies, being smaller at the higher energy. The experimental cross sections are larger by 35% at the higher energy, in agreement with the expected contribution from inelastic interactions. In the future, better np amplitudes may lead to a different conclusion, but based on the present results it does not appear likely. Also shown in Figs. 8(a) and 8(b) are the results for just the two IA diagrams combined (np and pp), and for all six graphs minus the one including two np interactions ($\nu=4$ in Fig. 7).

The results of the calculation for the analyzing power T_{20} are compared to the data in Figs. 9(a) and 9(b). Here again the results shown are for all graphs, all graphs minus the one with two np interactions, and for IA only (np and pp). It is obvious that the four rescattering graphs are much more important for T_{20} than for the cross section. In fact, the diagram with two np interactions gives unreasonable results compared to the data; we feel justified to remove it due to the great uncertainty of the np amplitude. Also shown is the analyzing power predicted by the simple geometric formula (5) above. It is not surprising that T_{20} is much more sensitive to the np amplitudes than the cross section; like other polarization

observables T_{20} results from a delicate balance of interfering amplitudes.

V. DISCUSSION AND CONCLUSION

In the IA framework the invariant differential cross section for inclusive breakup on hydrogen is

$$E_p d^2\sigma/p^2 dp\, d\Omega_p = m_N \sigma^{\text{total}}(np)|\Phi(q)|^2 , \quad (9)$$

where $\sigma^{\text{total}}(np)$ is the angle-integrated total np cross section. The detailed calculation in Sec. IV shows that this approximation is excellent; the full calculation differs from the IA value by ±5% at 1.25 GeV and ±20% at 2.0 GeV over most of the range of q allowed by the kinematics. The IA momentum density distribution $|\Phi(q)|^2$ derived from (9) for the 2.1-GeV data of this experiment are shown in Fig. 10. Also shown in Fig. 10 are the $|\phi(q)|^2$ values from a selection of ^{2}H$(p,2p)n$ data at 0.508 GeV (Ref. 5) and from the data of Aleshin *et al.*[24] at 1.0 GeV. The general agreement at low-q values, between the den-

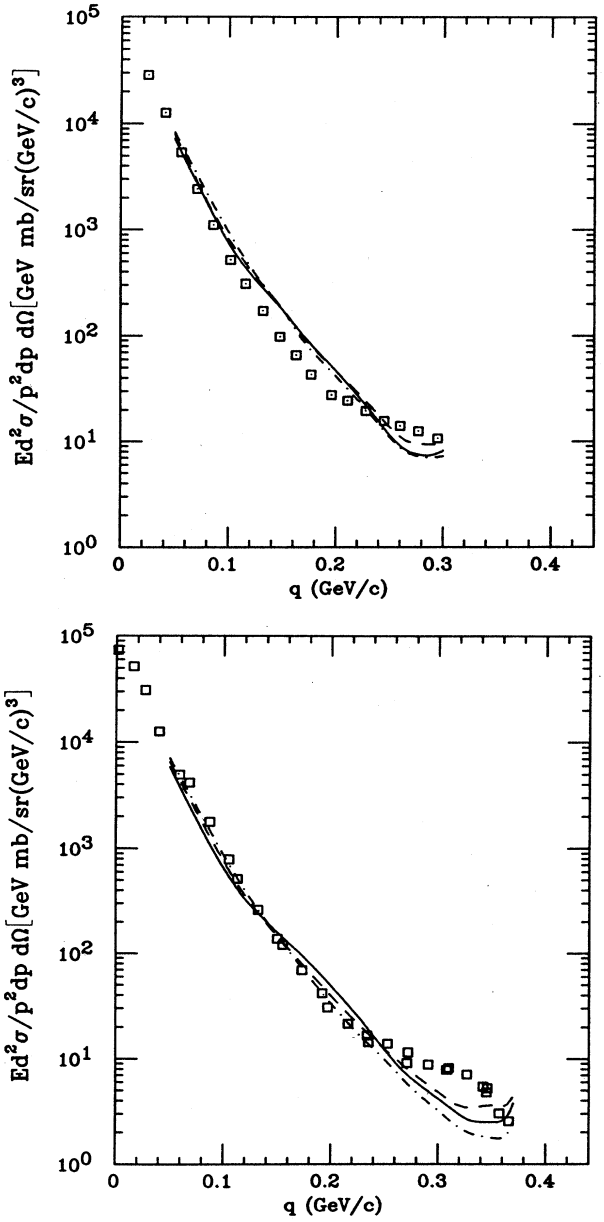

FIG. 8. (a) Differential cross section for ^{1}H at 1.25 GeV; the solid curve from all six graphs with Paris wave function and Arndt NN amplitudes. Dashed curve after removal of the second-order graph with two np interactions ($\nu=4$ in Fig. 7). Dot-dashed line for IA only, but for including both np and pp interactions. (b) Same as (a) but for the 2.1-GeV data; as explained in text, the curves have been calculated for 2.0 GeV.

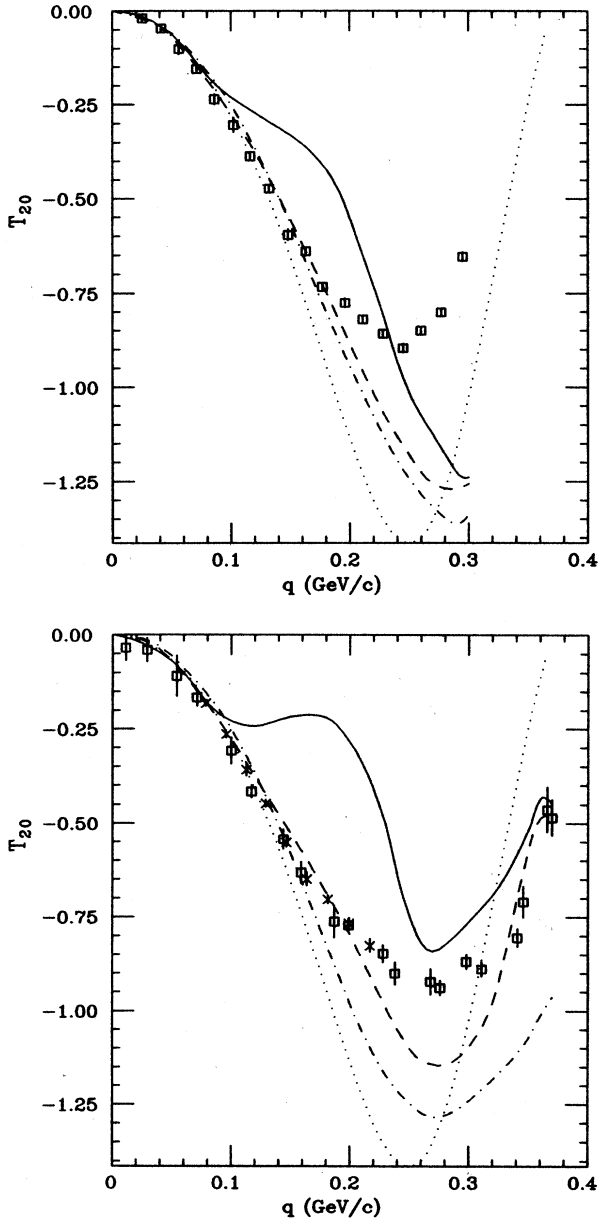

FIG. 9. (a) The T_{20} results for ^{1}H at 1.25 GeV; the curves have the same meaning as in Fig. 8. The dotted curve is for the geometric prediction with the Paris wave function. (b) Same as (a) for the 2.1-GeV data; again the theoretical prediction is for 2.0 GeV.

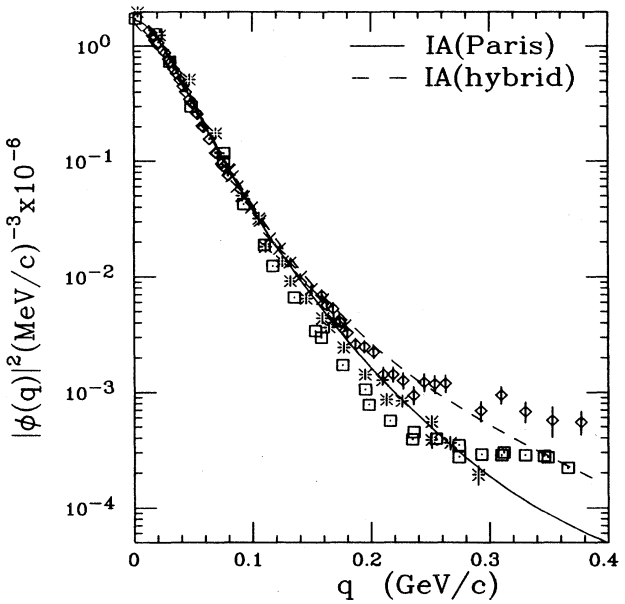

FIG. 10. Momentum density $|\Phi(q)|^2$ extracted from the ^{1}H$(d,p)X$ data at 2.1 GeV (□), compared with a selection from the 0.506 GeV ^{2}H$(p,2p)n$ data of Ref. 26 (◇), and the 1.0 GeV ^{2}H$(p,2p)n$ data of Ref. 24 (*). The solid curve is the geometric estimate with Paris wave function, and the dashed curve for hybrid wave function with the parameters of Ref. 3.

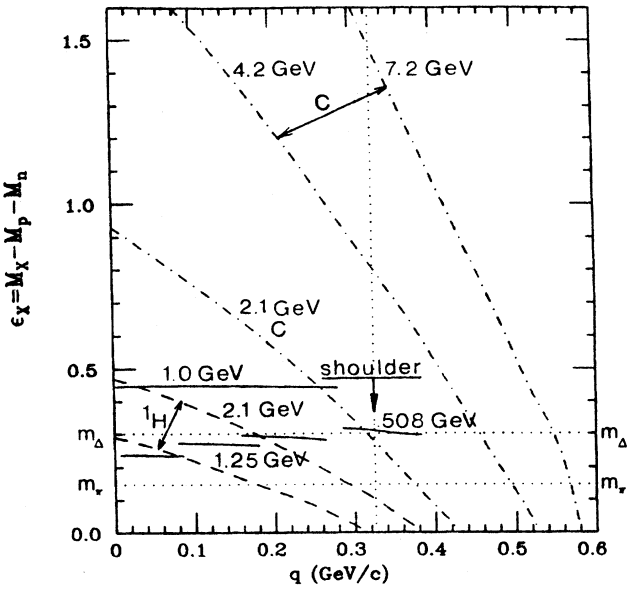

FIG. 11. Excitation energy vs q in the various $A(d,p)X$ experiments discussed; also included are the kinematical regions for the two $(p,2p)$ experiments from Refs. 26 and 24. The vertical dotted line indicated the position of the shoulder observed in the (d,p) experiments discussed here.

sity values extracted from the exclusive $(p,2p)$ and inclusive (d,p) data, is noteworthy. However, whereas the first two data sets show a flattening out of the momentum density starting just above $q=0.2$ GeV/c, the 1.0-GeV data of Ref. 24 do not show any change of slope, but continue along the IA prediction with the Paris wave function; most remarkable is the difference between the two $(p,2p)$ experiments. A similar flattening of the ^{1}H$(d,p)X$ cross section had also been noted by Fabbri *et al.*[25] for 1.62-GeV deuterons, starting at similar values of q; their results are not included here because the proton was not at 0°. In spite of this partial similarity in behavior near $q=0.3$ GeV/c, the fact that the 1.0 GeV $(p,2p)$ data do not follow the trend may give a clue concerning the origin of the deviation from the IA prediction.

In Fig. 11 the kinematical relationship between the excitation energy of a nucleon pair in either reaction is displayed as a function of q; for the $(p,2p)$ reaction q is assumed to be equal to the magnitude of the neutron recoil momentum. The excitation energy ϵ_x is defined by

$$\epsilon_x = M_x - m_p - m_n \ , \tag{10}$$

where the missing mass is $M_x^2=(E_d+m_H-E_p)^2-(\mathbf{d}-\mathbf{p})^2$ in (d,p); it is $M_x^2=(E_p+m_d-E_p')^2-(\mathbf{p}-\mathbf{p}')^2$ in $(p,2p)$, where $\mathbf{p}'$ is chosen to be the momentum of the proton which leads to the largest M_x value. In Fig. 11 the position of the anomalous shoulder in ^{12}C$(d,p)X$ at 7.2, 4.2, and 2.1 GeV (Dubna, Berkeley, and Saclay) is represented by the vertical dotted line. This is also the position of the similar, although stronger, shoulder seen in the present hydrogen data. The enormous difference in terms of excitation energy between the three experiments is dramatized in this figure. For the Dubna data (Ref. 1), $\epsilon_x \approx 1.45$ GeV at $q=0.325$ GeV/c, which is about ten times the pion mass. In contrast with this large number, $\epsilon_x \approx 0.27$ GeV in the present experiment and for ^{12}C, i.e., just below the excitation energy of the Δ, and at twice the mass of the pion. For the hydrogen data at both energies the shoulder is below pion threshold. Also shown in Fig. 11 are the values of ϵ_x for the $(p,2p)$ data shown in Fig. 10, at 1.0 GeV ($\epsilon_x \approx 0.45$ GeV) and 0.508 GeV ($\epsilon_x = 0.29$–0.31 GeV). It has been shown by Yano[26] that virtual excitation of the Δ could, as proposed by Aladashvili *et al.*[27], reproduce the experimental $(p,2p)$ cross section in the case of the large recoil data of Perdrisat *et al.*[28] (not shown in Figs. 10 and 11), for which the excitation energy in the proton pair is also near that of the Δ. It is possible, but not yet proven, that the 0.508 GeV $(p,2p)$ data shown in Fig. 10 are also strongly affected by Δ excitation. One would not expect the 1.0-GeV $(p,2p)$ data to be much affected by Δ excitation because $\epsilon_x = 0.45$ GeV, and this would explain the different behavior for the two sets of data illustrated in Fig. 10. In contrast to the situation with the $(p,2p)$ data, it is difficult to believe that Δ excitation could also generate the shoulder in all (d,p) data since the excitation energy is below pion threshold for the present data on ^{1}H, but high enough to excite half the nucleons of ^{12}C to the Δ resonance for the data of Ref. 1.

The shoulder seen at the same value of q and for various targets, and over a large range of energy can, of course, be interpreted as a manifestation of an intrinsic property of the deuteron. One apparent problem with

this interpretation is that the $(e,e'p)$ data of Bernheim *et al.*[29] do not show any structure near $q=0.3$ GeV/c. In the electron experiment the invariant mass of the np pair remains well below pion production threshold, as is the case in the ^{1}H$(d,p)X$ data, but unlike the ^{2}H$(p,2p)n$ TRIUMF data of Ref. 28. Excitation of a real Δ is thus not possible for the conditions of the $(e,e'p)$ experiment of Ref. 29 or the present ^{1}H(d,p) data. One might speculate that the striking difference between the Φ^2's from these two experiments is due to the different couplings of the photon and hadron to the "hidden color" component of the six-quark state in the deuteron; the existence of such a component has been discussed by Matveev and Sorba.[30]

A virtual $\Delta\Delta$ component may also exist at the level of a fraction of 1% in the deuteron, although attempts to detect it have been either ambiguous or inconclusive so far. Such a component would produce an enhancement at a q value corresponding to the maximum of its wave function, independently of whether or not pions are allowed in the final state by the kinematics selected in an experiment. One would, however, expect that such a component would be most visible when the Δ is on the mass shell and π decay is allowed by the experimental conditions, as for all ^{12}C$(d,p)X$ data. Yet it is in hydrogen that the shoulder is most prominent relative to the normal NN component. In Ref. 3 it was shown that a 5% $\Delta\Delta$ component in the $^7D_1$ state of angular momentum would be required in an IA calculation based on the Paris deuteron wave function, to reproduce the shoulder in the hydrogen data; the T_{20} data were not reproduced, even with such an unlikely strong $\Delta\Delta$ component.

Ableev *et al.*[1] have shown that the hybrid wave function of Kobushkin[31] could reproduce the shoulder in their data with a 4% component of a $|6q\rangle$ state added to the normal $|NN\rangle$ part of the deuteron wave function. In Ref. 3 it was shown that a slight change in the phase angle between the $|NN\rangle$ and $|6q\rangle$ components would reproduce both the differential cross section and T_{20} at 2.1 GeV for ^{12}C and hydrogen. The T_{20} prediction was based on the geometric form of the IA, formula (5); this prediction is shown again in Fig. 6 (a).

The momentum density distribution of the hybrid wave function is shown in Fig. 10 (dashed curve). It would be in general agreement with the data in this figure, with the exception of the 1.0-GeV $(p,2p)$ data. This point does not contradict the claim made above that the shoulders in (d,p) and $(p,2p)$ data have different origins, and thus appear at the same q value only by accident.

The point is further illustrated in Fig. 12 which shows the $|\Phi(q)|^2$ values extracted from the 7.2-GeV ^{12}C(d,p) data of Ref. 1 and from the 0.508-GeV ^{2}H$(p,2p)$ data of Ref. 5. Although the targets are different, the A independence shown by the present (d,p) data might justify the comparison. The two data sets in Fig. 12 show entirely different behaviors above $q=0.3$ GeV/c, differing by as much as a factor of 200 near $q=0.5$ GeV/c. Within the context of the various assumptions discussed above, the $|\Phi(q)|^2$ values in Fig. 12 reinforce the hypothesis of a different origin for the shoulders near $q=0.3$ GeV/c.

In conclusion, it has been shown that calculation of the

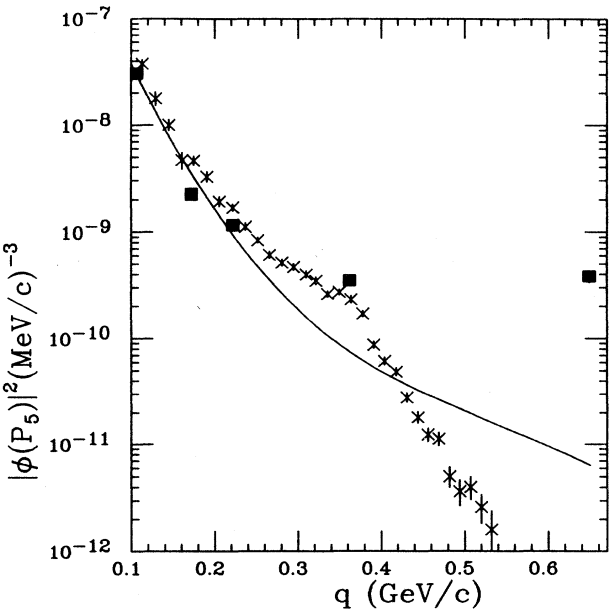

FIG. 12. Momentum density function $|\Phi(q)|^2$ extracted from the ^{12}C$(d,p)X$ data of Ableev *et al.* at 7.2 GeV ($\times$) and from the 0.508 GeV ^{2}H$(p,2p)$ experiments of Ref. 26 (■). The solid curve is the Paris deuteron wave-function density.

six lowest-order graphs contributing to ^{1}H$(d,p)n$ did not explain the shoulder in the hydrogen data presented here. Although the T_{20} data on hydrogen show a surprising energy independence, suggesting applicability of the IA, the calculation underestimates the analyzing power. This failure of the calculation could be an artifact of the np phase-shift amplitudes used here. The omnipresence of the shoulder in the breakup differential cross section remains puzzling, as it is suggestive of an intrinsic property of the deuteron. Likewise, the near energy independence of T_{20} in ^{12}C$(d,p)X$ suggested by the data of Ref. 16 and the present ones, reinforce this suggestion. Yet no similar shoulder is seen in the existing $(e,e'p)$ data.

A detailed elucidation of the apparent irreconcilabilities between the data of the three different experiments, exclusive ^{2}H$(p,2p)n$ and ^{2}H$(,e,e'p)n$, and inclusive $A(d,p)X$, will have to await further theoretical work. The two exclusive reactions give different but compatible information: for the first the excitation of the Δ is likely to be at the origin of the shoulder near $q=0.30$ GeV/c; no shoulder is seen in the second and none would be expected from Δ excitation because $\epsilon_x < m_\pi$. The inclusive data from this and the higher-energy experiments on ^{1}H and heavier targets do not indicate an obvious connection with Δ excitation. The strongest shoulder is in ^{1}H at 2.1 GeV, where $\epsilon_x < m_\pi$.

The most interesting features of the $A(d,p)X$ reaction are the universal presence of a shoulder at a constant value of the proton momentum in the deuteron rest frame, q, over a large range of energy and A values and the indication of a similar universality for T_{20}, which is also independent of energy and target A value. The new data presented here will hopefully stimulate theoretical

activity which will lead to an explanation of the origin of this universality.

ACKNOWLEDGMENTS

We are thankful for the efficient and dedicated work of the Saturne staff which provided excellent beams for this experiment. We also recognize the help provided by B. Arapoglou (Orsay) and J. Berger in the earlier phase of this experiment. Partial funding for four of us (V.P., C.F.P., P.U., and C.L.) was provided by the U.S. National Science Foundation, with Grant PHY85-09880.

---

*Present address: Norfolk State University, Norfolk, Virginia 23504.

[1]V. G. Ableev, D. A. Abdushukurov, S. A. Avramenko, Ch. Dimitrov, A. Filipkowski, A. P. Kobushkin, D. K. Nikitin, A. A. Nomofilov, N. M. Piskunov, V. I. Sharov, I. M. Sitnik, E. A. Strokovsky, L. N. Strunov, L. Vizireva, G. G. Vorobiev, and S. A. Zaporozhets, Nucl. Phys. **A393**, 491 (1983); Pis'ma Zh. Eksp. Teor. Fiz. **37**, 196 (1983) [JETP Lett. **37**, 233 (1983)].

[2]L. Anderson, W. Bruckner, E. Moeller, S. Nagamiya, S. Nissen-Meyer, L. Schroeder, G. Shapiro, and H. Steiner, Phys. Rev. C **28**, 1224 (1983).

[3]C. F. Perdrisat, V. Punjabi, C. Lyndon, J. Yonnet, R. Beurtey, M. Boivin, A. Boudard, J. P. Didelez, R. Frascaria, T. Reposeur, R. Siebert, E. Warde, F. Plouin, P. C. Gugelot, and J. Y. Grossiord, Phys. Rev. Lett. **59**, 2840 (1987).

[4]L. L. Frankfurt and M. I. Strikman, Nucl. Phys. **B148**, 107 (1979).

[5]V. Punjabi, K. A. Aniol, A. Bracco, C. A. Davis, M. B. Epstein, H. P. Gubler, J. P. Huber, W. P. Lee, D. J. Margaziotis, C. F. Perdrisat, P. R. Poffenberger, H. Postma, H. J. Sebel, A. W. Stetz, and W. T. H. van Oers, Phys. Rev. C **38**, 2728 (1988).

[6]R. A. Arndt, L. D. Roper, R. A. Bryan, R. B. Clark, B. J. VerWest, and P. Signell, Phys. Rev. D **28**, 97 (1983); phase shifts from SAID SP88 0–1.3 GeV; R. A. Arndt, J. S. Hyslop III, and L. D. Roper, Phys. Rev. D **35**, 128 (1988).

[7]R. A. Arndt, Phys. Rev. D **37**, 2665 (1988).

[8]J. Bystricky, C. Lechanoine-Leluc, and F. Lehar, J. Phys. (Paris) **48**, 199 (1987).

[9]M. A. Ignatenko and G. I. Lykasov, Yad. Fiz. **46**, 1080 (1987) [Sov. J. Nucl. Phys. **46**, 625 (1987)].

[10]L. S. Azhgirei, I. K. Vzorov, V. N. Zhmyrov, V. V. Ivano, M. A. Ignatenko, A. S. Kuznetsov, Yu. A. Kozhevnikov, E. Mulas, S. V. Razin, G. D. Stoletov, and N. P. Yudin, Yad. Fiz. **46**, 1194 (1987) [Sov. J. Nucl. Phys. **46**, 661 (1987)].

[11]E. Grorud, J. L. Laclare, A. Ropert, A. Tkatchenko, J. Banaigs, and M. Boivin, Nucl. Instrum. Methods **188**, 549 (1981).

[12]M. Bedjidian, D. Contardo, E. Descroix, S. Gardien, J. Y. Grossiord, A. Guichard, M. Gusakow, R. Haroutunian, M. Jacquin, J. R. Pizzi, D. Bachelier, J. L. Boyard, T. Hennino, J. C. Jourdain, M. Roy-Stephan, and P. Radvanyi, Nucl. Instrum. Methods **A257**, 132 (1987).

[13]R. Frascaria *et al.*, in *Medium Energy Nucleon and Antinucleon Scattering*, Vol. 243 of *Springer Lecture Notes in Physics*, edited by H. V. von Germab, (Springer-Verlag, Berlin, 1985), p. 541.

[14]J. Arvieux, S. D. Baker, R. Beurtey, M. Boivin, J. M. Cameron, T. Hasegawa, D. Hutcheon, J. Banaigs, J. Berger, A. Codino, J. Duflo, L. Goldzahl, F. Plouin, A. Boudard, G. Gaillard, Nguyen Van Sen, and Ch. F. Perdrisat, Nucl. Phys. **A431**, 613 (1984); J. Arvieux, S. D. Baker, A. Boudard, J. Cameron, T. Hasegawa, D. Hutcheon, C. Kerboul, G. Gaillard, and N. van Sen, Nucl. Instrum. Methods (to be published).

[15]R. Vinh Mau, in *Mesons in Nuclei*, edited by M. Rho and D. Wilkinson (North-Holland, Amsterdam, 1979), p. 151.

[16]V. G. Ableev, S. V. Dshemuchadze, S. V. Fedukov, V. V. Fimushkin, A. D. Kirillov, A. P. Kobushkin, V. I. Kotov, B. Kuehn, P. K. Manyakov, V. A. Monchinsky, B. Naumann, L. Naumann, W. Neubert, A. A. Nomofilov, S. A. Novikov, L. Penchev, J. K. Philipenko, N. M. Piskunov, P. A. Rukoyatkin, V. I. Sharov, I. M. Sitnik, E. A. Strokovsky, L. N. Strunov, A. L. Svetov, L. Vizireva, V. I. Volkov, and S. A. Zaporozhets, Pis'ma Zh. Eksp. Teor. Fiz. **49**, 558 (1988).

[17]J. M. Wallace, Phys. Rev. C **5**, 609 (1972).

[18]R. G. Glauber, in *Lectures in Theoretical Physics*, edited by W. E. Brittin and L. G. Dunham (Interscience, New York, 1959), Vol. I, p. 315.

[19]V. Punjabi, Ph.D. thesis, College of William and Mary, 1986.

[20]V. Punjabi, C. F. Perdrisat, W. T. H. van Oers, P. R. Poffenberger, W. P. Lee, C. A. Davis, A. Bracco, D. J. Margaziotis, J. P. Huber, M. B. Epstein, H. Postma, H. J. Sebel, and A. W. Stetz, Phys. Lett. B **179**, 207 (1986).

[21]M. Lacombe, B. Loiseau, R. Vinh Mau, J. Cote, P. Pires, and R. de Tourreil, Phys. Lett. **101B**, 139 (1981).

[22]H. P. Stapp, T. Ypsilantis, and N. Metropolis, Phys. Rev. **105**, 302 (1957).

[23]F. Udo, Rev. Mod. Phys. **37**, 365 (1965).

[24]N. P. Aleshin, S. L. Belostotsky, Yu. V. Dotsenko, O. G. Grebenyuk, L. M. Kochenda, L. G. Kudin, N. P. Kuropatkin, S. I. Manayenkov, O. V. Miklukho, V. N. Nikulin, O. E. Prokofjev, A. Yu. Tsaregorodtsev, S. S. Vokov, J. Ero, J. Kecskemeti, Zs. Kovacs, and Z. Seres, University of Leningrad Report 1259, 1987.

[25]F. L. Fabbri, A. Malecki, P. Picozza, J. Banaigs, J. Berger, L. Goldzahl, L. Vu Hai, M. Cottereau, and C. Le Brun, Lett. Nuovo Cimento **17**, 21 (1976).

[26]A. F. Yano, Phys. Lett. **156B**, 33 (1985).

[27]B. S. Aladashvili, J.-F. Germond, V. V. Glagolev, M. S. Nioradze, T. Siemiarczuk, J. Stepaniak, V. N. Streltsov, C. Wilkin, and P. Zielinski, J. Phys. G **3**, 1225 (1977).

[28]C. F. Perdrisat, V. Punjabi, M. B. Epstein, D. J. Margaziotis, A. Bracco, H. P. Gubler, W. P. Lee, P. R. Poffenberg, W.T.H. van Oers, Y. P. Zhang, H. Postma, H. J. Sebel, and A. W. Stetz, Phys. Lett. **156B**, 38 (1985).

[29]M. Bernheim, A. Bussiere, J. Mougey, D. Royer, D. Tarnowski, S. Turck-Chieze, S. Frullani, G. P. Capitani, E. de Sanctis, and J. Jans, Nucl. Phys. **A365**, 349 (1981).

[30]V. A. Matveev and P. Sorba, Lett. Nuovo Cimento **20**, 435 (1977).

[31]A. B. Kobushkin and L. Vizireva, J. Phys. G **8**, 893 (1982).